

Paper published in:

J. Mendes, D. Gallipoli, F. Boeck and A. Tarantino (2020).

A comparative study of high capacity tensiometer designs.

Physics and Chemistry of the Earth, 120: 102901

<https://doi.org/10.1016/j.pce.2020.102901>

<b>Title:</b>	A comparative study of high capacity tensiometer designs
<b>Keywords:</b>	High capacity tensiometers, soil suction, laboratory testing

	<b>Author</b>	<b>Affiliation</b>	<b>Email Address</b>
<b>1</b>	<b>Joao Mendes*</b>	Department of Mechanical & Construction Engineering, Northumbria University, United Kingdom	joao.mendes@northumbria.ac.uk
<b>2</b>	<b>Domenico Gallipoli</b>	Dipartimento di Ingegneria civile, chimica e ambientale (DICCA), Università degli Studi di Genova , Italy Formerly, Laboratoire SIAME, Fédération IPRA, Université de Pau et des Pays de l'Adour, France	domenico.gallipoli@unige.it
<b>3</b>	<b>Flora Boeck</b>	Formerly UMS - METER Group AG, Germany	floralisaboeck@gmail.com
<b>4</b>	<b>Alessandro Tarantino</b>	Department of Civil and Environmental Engineering, University of Strathclyde, United Kingdom	alessandro.tarantino@strath.ac.uk

\* - **Corresponding author:**

**Address:**

Northumbria University  
Faculty of Engineering and Environment  
Department of Mechanical & Construction Engineering  
Wynne Jones Building, Room 117  
Newcastle upon Tyne, NE1 8ST  
United Kingdom

**E-mail:**

joao.mendes@northumbria.ac.uk

**Highlights:**

- *The suction measuring range of seven distinct high capacity tensiometer prototypes has been compared*
- *Larger air entry value of the porous filter increases the suction measurement range*
- *The air entry value is inversely related to the size of largest pore in the porous filter*
- *Water reservoir size and protective casing have little influence on the suction range*
- *The application of larger water pressures during saturation increases the suction range*

# A comparative study of high capacity tensiometer designs

**Mendes J., Gallipoli D., Boeck F., Tarantino A.**

## **Abstract**

The High Capacity Tensiometer (HCT) is a soil sensor that can measure large negative pore-water pressures, i.e. in excess of -1 MPa, and is a key instrument for monitoring ground-atmosphere interactions. The design of HCTs has not changed since the first prototype was proposed in the 1990s and still includes three main components, namely a high air-entry value porous filter, a small water reservoir and a pressure transducer, which are all encased inside a protective sheath. Despite many successful examples of measurement of pore-water tension in the laboratory and the field, there are essentially no commercially available HCTs for industrial applications. The rare utilisation of HCTs in engineering practice has always relied on bespoke devices that have been purposely designed by research laboratories or suppliers of soil sensors. The dissemination of HCTs into engineering practice has been further hindered by the relatively poor understanding of sensor design and its impact on the reliability of measurements. To overcome such gap of knowledge, this paper explores the influence of distinct design variables (i.e. the porous filter, the pressure transducer, the water reservoir size and the protective casing) on the measuring range of HCTs. Seven prototypes were manufactured with different combinations of the above design variables showing that, if HCTs are properly saturated, the air entry value of the filter has the strongest influence on the measuring range while the effects of reservoir size, pressure transducer and protective casing are relatively modest. It is expected that the results from this work will guide future design of HCTs, thus contributing to the development of resilient sensors for geotechnical applications.

## **Keywords**

High capacity tensiometers, pore-water tension, soil suction.

## 1 Introduction

Natural soils and geotechnical infrastructure (e.g. road/railway/flood embankments and earth dams) are strongly affected by evapotranspiration and the consequent occurrence of capillary (tensile) water close to the ground surface. In the vadose region, pore-water pressures are negative and soil suction is defined as the difference between pore-air and pore-water pressure which means that, under atmospheric conditions, soil suction coincides with the negative pore-water pressure changed of sign.

A number of instruments are commercially available to measure negative pore-water pressures in soils and, among these, the most common options are conventional tensiometers and porous block sensors. Conventional tensiometers provide a direct measurement of negative pore-water pressures over a relatively limited range of values, from 0 to -80 kPa, which is often exceeded in the field especially during dry spells. Instead, porous block sensors provide an indirect record of negative pore-water pressures based on the measurement of the electrical or thermal properties of a porous element in contact with the soil. Porous block sensors are generally unsuitable for geotechnical applications as they suffer from a slow response time and poor accuracy. For example, they are unable to capture the rapid changes of soil suction caused by the fast propagation of a water front during rainwater infiltration.

In contrast with commercial devices, the High Capacity Tensiometer (HCT) is a sensor that can measure large pore-water tensions, well beyond the water cavitation threshold of -100 kPa, with a relatively quick response and good accuracy. The first HCT prototype was developed by Ridley and Burland (1993) and measured negative pore-water pressures in excess of -1500 kPa. This pioneering work provided the basis for the subsequent design of a number of HCT prototypes by different research groups around the world (Guan and Fredlund, 1997; Marinho and de Sousa Pinto, 1997; Tarantino and Mongiovi, 2002; Meilani et al., 2002; Take and Bolton, 2003; Toker et al., 2004; Lourenco et al., 2008; Cui et al., 2008; Mendes and Buzzi, 2014; Bagheri et al., 2018). The reader may refer to Marinho et al. (2008) for a review of the theoretical and practical aspects of suction measurement by means of HCTs.

To date, HCTs have been used in the field to monitor pore-water pressures inside slopes or agricultural soils (Mendes et al., 2008, Cui et al. 2008, Toll et al. 2011) but also in the laboratory to measure the changes of suction during oedometer tests (Tarantino and De Col 2008; Le et al. 2011; Wijaya and Leong, 2016), direct shear tests (Caruso and Tarantino, 2004) and triaxial tests (Cunningham et al. 2003; Mendes and Toll, 2016). Past studies have always made use of bespoke devices that have been purposely designed and manufactured by research laboratories and suppliers of soil sensors. Two main concept of HCT design have been put forward over the years: in one case, the HCT incorporates a strain gauge pressure transducer that forms an integral part of the sensor body (Tarantino and Mongiovi, 2002) while, in the other case, the HCT consists of the assembly of a commercial pressure transducer and a porous filter, which are glued with an epoxy resin inside a protective casing (Delage et al., 2008). The former design concept has the advantage of minimizing the number of connections between parts and therefore reduces the potential entrapment of air cavitation nuclei. This design is however difficult to manufacture and suffers from high temperature sensitivity, which makes it unsuitable for field use. The latter design concept overcomes these limitations while preserving a good measuring performance (Delage et al., 2008) and is therefore the preferred choice for industrial applications.

In spite of many successful examples of suction measurement in the laboratory and in the field, there are no commercially available HCTs for routine engineering applications. The dissemination of HCTs beyond the academic context has also been impeded by a relatively poor understanding of sensor design in relation to measuring performance. To overcome this limitation, the present paper investigates the measuring range of seven different HCT prototypes manufactured according to the latter of the above two design concepts. The study analyses different combinations of porous filters, pressure transducers, water reservoir sizes and protective casings to identify their effect on the sensor measuring range. The procedures for saturating HCTs are also briefly discussed in the paper. The objective is to highlight the advantages and disadvantages of different prototypes in order to support the future design of HCTs that may attract the interest of geotechnical practitioners.

## 2 Background

Figure 1 shows the first HCT developed in the 1990s at the Imperial College, London, by Ridley and Burland (1993). Since then, the design of HCTs has changed relatively little and it still comprises the following three main components: a) a high air entry value porous filter which is typically made of ceramic, b) a small water reservoir with a capacity between  $10 \text{ mm}^3$  and  $100 \text{ mm}^3$  and c) a pressure transducer, which may consist of either an integral strain gauge diaphragm or an off-the-shelf commercial device.

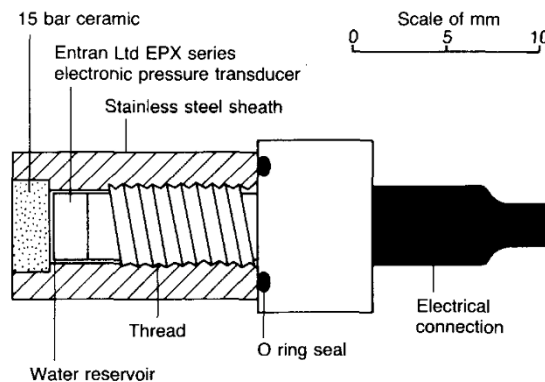


**Figure 1.** Imperial College HCT (Ridley and Burland, 1993).

After saturation of the HCT with water, the outer face of the porous filter is placed in contact with the soil whose suction will be measured. The porous filter has therefore the purpose of ensuring the hydraulic continuity between the water inside the HCT reservoir and the soil. Mendes et al. (2015) suggested that, among all design components, the porous filter has the strongest influence on the maximum water tension that can be sustained by the HCT (i.e. the measuring range of the HCT). Indeed, the Air Entry Value (AEV) of the porous filter often coincides with the maximum water tension that a HCT can measure. For example, this is the case for the HCT shown in Figure 1 which, according to Ridley and Burland (1993), measured a maximum pore-water tension of about  $-1500 \text{ kPa}$  that is consistent with the 15 bar AEV of the ceramic filter. This would imply that, if the ceramic filter is in contact with a saturated clay having an air-entry suction greater than the AEV of the filter, the maximum suction measured by the tensiometer would coincide with the air-entry suction of the clay rather than the AEV of the filter. Nevertheless, this aspect has never been investigated experimentally in detail.

The purpose of the water reservoir is to allow the small inwards deflection of the transducer diaphragm during suction measurements. Past evidence suggests that the size of the water reservoir does not influence the measuring range of the sensor (Mendes and Buzzi, 2013), though a large reservoir might undermine the long-term stability of measurements (Mendes and Gallipoli, 2020).

The external casing protects the filter, the pressure transducer and the water reservoir from the application of external loads, which could generate additional deformations of the sensing diaphragm and, hence, produce spurious measurements of water pressure. External loads may be caused by mechanical actions during installation and measurement but also by the different thermal expansion/contraction of the casing and pressure transducer. These effects cannot be accounted for by zeroing the readings before installation with the HCT under stress-free conditions and at a constant ambient temperature, because these conditions differ from those inside the ground. Particular care should therefore be taken when choosing the material and the geometry of the protective casing so as to minimize the occurrence of spurious measurements. Reading inaccuracies are more likely to occur if the sensing diaphragm is an integral part of the sensor body.

Finally, adequate procedures should be adopted to minimise the air trapped inside the reservoir and filter during saturation of HCTs because the presence of gas nuclei may induce errors in measurements, reduce

the maximum sustainable suction and undermine the stability of readings over time (Mendes and Gallipoli, 2020).

### 3 Design of HCT prototypes

The seven prototypes investigated in the present work were designed and manufactured with: a) two different ceramic filters presenting distinct mineralogical compositions and pore size distributions, b) two different pressure transducers with distinct geometries, i.e. a flush diaphragm transducer and a cavity diaphragm transducer, c) two different water reservoir sizes (corresponding to the different pressure transducer geometries) and d) two different protective casings made of stainless steel and ceramic.

#### 3.1 Ceramic filters

Among all design components, the AEV of the filter has the strongest influence on the maximum water tension that can be sustained by HCTs. The AEV is the maximum difference that can exist between the air and water pressures acting on the two sides of a saturated filter (with the former being larger than the latter) without allowing the air to break through the filter. During field measurements, the air pressure on the external face of the HCT filter is atmospheric while the water inside the reservoir is under tension. Note that this is unlike the measurement of the AEV in the laboratory where the air pressure on one side of the saturated filter is usually bigger than atmospheric while the water pressure on the other side is atmospheric.

The above pressure difference can be sustained by the saturated filter thanks to the formation of concave water menisci on the side of the filter that is exposed to the air. These menisci act as a “membrane”, which separates the air from the water up until the attainment of the maximum possible pressure difference, i.e. the AEV of the filter. Once this limit is exceeded, the air penetrates inside the filter as a separate phase causing the desaturation of the HCT and the consequent breakdown of suction measurements. The AEV of the filter therefore constitutes an upper bound of the maximum suction that can be measured by HCTs.

The AEV is inversely related to the size of the largest pore inside the filter, which means that smaller pore sizes correspond to greater AEVs and therefore to greater maximum sustainable water tensions. This is also consistent with the predictions of the Young-Laplace equation which, under the simplifying hypothesis of cylindrical pores, shows that the AEV is inversely proportional to the largest pore diameter,  $d_{max}$ :

$$AEV = \frac{4 \sigma_w \cos \theta_w}{d_{max}} \quad [1]$$

where,  $\sigma_w$  is the air-water surface tension (72.8 mN/m at 293 °K) and  $\theta_w$  is the contact angle between the filter material and the water. Note that, if the material of the filter is perfectly wettable, the contact angle is equal to zero.

Two different ceramic filters were used in this work, namely a kaolinite ceramic filter (herein named KCF) and an alumina ceramic filter (herein named ACF), which exhibit different mineralogical compositions and porosity characteristics. The porosity characteristics of the two filters were measured by means of Mercury Intrusion Porosimetry (MIP) and Nitrogen Adsorption (NA) tests, which detect voids of different sizes. MIP tests determine the pore size distribution over the large void range from 7 nm up to 0.5 mm while NA tests determine the pore size distribution over the small void range from 2 nm to 50 nm. The results from the two tests must therefore be combined to achieve a full characterization of the pore-size distribution of the material.

In MIP tests, the pore volume is determined from the amount of intruded mercury under a given pressure,  $P$  while the corresponding pore diameter,  $d_{pore}$  is calculated from the Young-Laplace equation as:

$$d_{pore} = \frac{4 \sigma_m \cos \theta_m}{P} \quad [2]$$

where,  $\sigma_m$  is the air-mercury surface tension (here assumed equal to 485 mN/m at 293 °K) and  $\theta_m$  is the contact angle between the filter material and the mercury (here assumed equal to 130°). In NA tests, the pore size distribution is determined by measuring the adsorption and desorption of nitrogen on the pore surface at different relative pressures and at a constant temperature of 77 °K, according to the method proposed by Barret et al. (1951).

Figure 2 shows that the KCF and ACF exhibit markedly different porosity characteristics in terms of both volume and sizes of voids. In particular, the KCF exhibits a polydisperse porosity distribution over a range of relatively small diameters (from 2 nm to 220 nm), with a peak at around 65 nm. Conversely, the ACF exhibits a monodisperse distribution over a range of larger diameters (from 100 nm to 290 nm), with a peak at around 230 nm. Each MIP and NA test was repeated twice, except for the MIP test on the ACF that was repeated three times, to validate the correctness of the adopted laboratory procedures.

Equation 1 was used to estimate the theoretical AEV of both filters based on the measured porosity characteristics. The largest pore size of the KCF is comprised between 165 nm and 220 nm, which corresponds to a theoretical AEV between 1.3 MPa and 1.7 MPa according to Equation 1 (if the filter is assumed to be perfectly wettable, i.e.  $\theta_w = 0^\circ$ ). This calculation matches well the nominal AEV of the ceramic filter, which is equal to 1.5 MPa (15 bar) according to technical documentation provided by the supplier. For ease of interpretation, Figure 2 also shows the pore diameter calculated from Equation 1 in correspondence of the nominal AEV of 1.5 MPa (15 bar), which matches well the upper limit of the MIP curve. Conversely, the largest pore size of the ACF is comprised between 250 nm and 290 nm, which is considerably larger than the largest pore size of the KCF and corresponds to a theoretical AEV between 1.0 MPa and 1.1 MPa according to Equation 1 (if the filter is assumed to be perfectly wettable, i.e.  $\theta_w = 0^\circ$ ). In this case, however, no nominal AEV was provided by the filter supplier, though air-breakthrough experiments indicated that the AEV should be comprised between 0.7 and 1.0 MPa (7 and 10 bar respectively). Once again, Figure 2 shows the pore diameter calculated from Equation 1 in correspondence of an AEV of 1 MPa (10 bar), which matches well the upper limit of the MIP curve.

Table 1 summarizes the different characteristics of the two ceramic filters in terms of porosity, specific density and bulk density. Inspection of Table 1 indicates that the ACF exhibits a significantly lower porosity and a considerably higher specific density than the KCF, which results in a higher bulk density. These characteristics are also consistent with the significantly higher levels of strength and hardness of the ACF compared to the KCF.

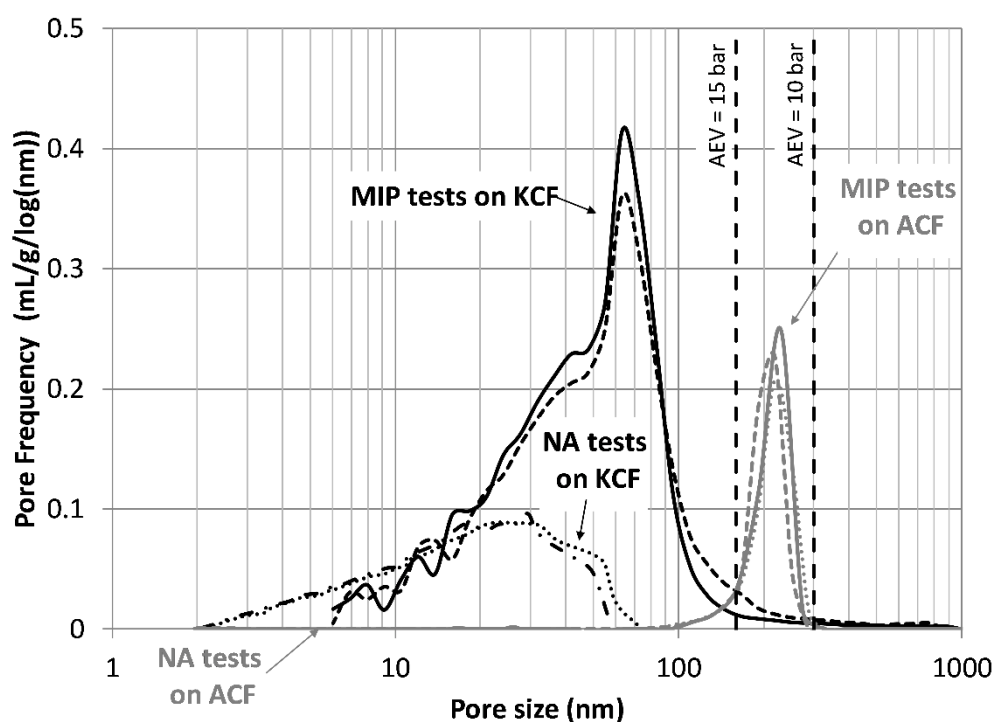


**Figure 2.** Pore size distribution of KCF and ACF measured by means of mercury intrusion porosimetry (MIP) and nitrogen adsorption (NA) tests.

**Table 1.** Ceramic filter properties.

	Pore size range nm	Largest pore nm	Porosity %	Specific density g/cm <sup>3</sup>	Bulk density g/cm <sup>3</sup>
KCF	2 - 220	165 - 220	33	2.02	1.35
ACF	100 - 290	250 - 290	13	3.10	2.70

### 3.2 Pressure transducers

The pressure transducer range should be equal to at least the AEV of the filter in order to exploit the full measuring potential of the HCT. The transducer must also be capable of recording both positive (compressive) and negative (tensile) water pressures to maximize sensor versatility but also to allow calibration. This is because calibration is normally performed in the positive pressure range and then extrapolated to the negative pressure range by assuming a symmetric response of the sensing diaphragm (Tarantino and Mongioví, 2002). A unique linear correlation is therefore assumed between transducer voltage and applied pressure, regardless of whether the sensing diaphragm is deforming towards the reservoir (if water pressure is negative) or away from the reservoir (if water pressure is positive). This assumption could be validated by imposing a positive pressure at the back of the sensing diaphragm (Tarantino and Mongioví, 2003), though this check is not commonly performed during HCT design.

Two different pressure transducers were used in this work, namely a ceramic cavity diaphragm transducer (herein named CD) and a ceramic flush diaphragm transducer (herein named FD), which are both depicted



in Figure 3. These transducers are made of 96% pure alumina and their characteristics are summarized in Table 2.

Both transducers have a full scale (FS) of 2000 kPa in the positive pressure range, though no information is provided by the manufacturer about their ability to measure negative pressures. Technical documentation also indicates a measurement accuracy equal to 0.5% of the full scale, which corresponds to an error margin of  $\pm 10$  kPa. Therefore, a small full scale is preferable to maximize transducer accuracy, though a large full scale is often necessary to apply high positive pressures that can dissolve all residual air nuclei during the saturation of HCTs prior to use. A full scale of 2000 kPa has here been chosen as a compromise between these two opposite requirements as it provides a good accuracy of  $\pm 10$  kPa while allowing the application of a saturation pressure up to 4000 kPa. This very large value is admissible because the transducer performance is compromised only when the applied pressure attains the overpressure limit of the device, which is twice its full scale range. In this work, a saturation pressure of about 3000 kPa was chosen because this value is two times greater than the AEV of the filter and is considered sufficient to achieve an adequate dissolution of most residual air nuclei.

Another CD ceramic transducer, with a smaller measuring range of 500 kPa, was also used to achieve a higher accuracy of  $\pm 2.5$  kPa at the price, however, of a lower pre-pressurisation which is likely to limit the maximum sustainable water tension.

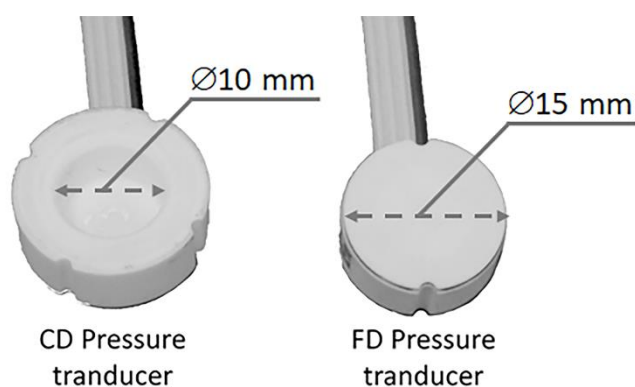


**Figure 3.** Ceramic cavity diaphragm (CD) pressure transducer (left) and ceramic flush diaphragm (FD) pressure transducer (right).

**Table 2.** Pressure transducer characteristics.

Designation	Ceramic flush diaphragm	Ceramic cavity diaphragm
Short name	FD	CD
Sensor type	Piezoresistive	
Pressure reference	Relative to atmosphere	Relative to atmosphere
Pressure full scale range (FS) [kPa]	2000	500 / 2000
Accuracy [%FS]	0.5	

### 3.3 Water reservoir

The purpose of the water reservoir is to create a gap between the ceramic filter and the flexible diaphragm of the pressure transducer, so that no contact occurs between these two components when the latter deflects inwards during measurements of negative pore-water pressures. Two groups of HCT prototypes were manufactured in this work to incorporate gaps of different sizes between the ceramic filter and the pressure transducer. One group incorporates a small water reservoir, which is delimited by the flush diaphragm (FD) transducer at the base and by the protective casing on the sides, thus resulting in a capacity of only 40 mm<sup>3</sup>. Another group incorporates a large water reservoir defined by the shape of the cavity diaphragm (CD) transducer which delimits both the base and the sides of the reservoir, thus resulting in a capacity of about 430 mm<sup>3</sup>. The details of the design of all HCT prototypes are discussed later in the paper.

The above transducer choices were aimed to investigate the effect of the water reservoir size on both the measuring range and the long-term stability of measurements. The former effect is discussed in the present paper while the latter effect is considered elsewhere (Mendes and Gallipoli, 2020).

### 3.4 Protective casing

The protective casing must be stiff enough to minimize any transfer of stresses to the transducer as this may generate spurious measurements of pressure. The casing must also be chemically inert, i.e. it must not react with water or any other compound commonly found in soils. This aspect is particularly important if the water inside the reservoir is in direct contact with the inner surface of the casing. Finally, the casing should exhibit a low thermal expansion/contraction coefficient to avoid the application of stresses to the sensing unit as a consequence of temperature fluctuations, which are particularly frequent in field applications. The utilization of epoxy glue may also contribute to the generation of internal stresses because of the different thermal expansion coefficients of the pressure transducer and the epoxy that binds it (Toker et al., 2004).

Two types of protective casings were manufactured in the present work by using two different materials, namely stainless steel 316 (herein named SS316) and 99% pure alumina ceramic (herein named Al). These materials are very stiff and chemically inert, which satisfies the first two of the above three requirements. As for thermal behaviour, however, both materials exhibit temperature-induced deformations, which potentially poses a problem to the accuracy of measurements. Table 3 shows the main properties of the two materials and indicates that alumina ceramic is preferable to stainless steel as it exhibits a smaller thermal expansion coefficient, a higher specific heat and a higher stiffness. A higher specific heat means that the material must exchange a larger amount of energy with the surrounding environment to attain a given change of temperature. A higher specific heat therefore corresponds to a larger thermal inertia and consequently to smaller temperature changes of the casing material, which is of course a desirable property. Unfortunately, temperature-induced deformations cannot be eliminated and their effect on suction measurements should be compensated based on calibration at different temperatures. This is particularly important in field applications as, in this case, thermal fluctuations are more significant than in a controlled laboratory environment.

The process of manufacture of the casing is also different depending on the chosen material, namely stainless steel casings are machined out of solid rods while ceramic casings are casted to shape. In the former case, fine geometric details such as threads, grooves or ridges can be included with relative ease and mistakes can be generally rectified at a later stage. In the latter case, the casing geometry must be as straightforward as possible because of the moulding process, which only allows for the inclusion of simple details and makes virtually impossible any modification after casting.

**Table 3.** Main properties of casing materials.

		SS316	Al
<b>Thermal coefficient of linear expansion</b>	<b>[10<sup>-6</sup> K<sup>-1</sup>]</b>	16	8
<b>Thermal conductivity at 25°C</b>	<b>[W/(m.K)]</b>	16	35
<b>Specific heat</b>	<b>[J/(kg.K)]</b>	500	880
<b>Stiffness (Young modulus)</b>	<b>GPa</b>	200	360

### 3.5 HCT prototype designs

Table 4 shows the five HCT designs developed in the present work. Two of these designs were implemented in two different versions, using different ceramic filters and pressure transducers, which gives a total of seven HCT prototypes. All prototypes have a cylindrical shape with a length between 35 and 60 mm and a diameter of about 26 mm. The prototypes are named according to the format VVV – WW(XXXX) – YYYYY [Z], which describes the different design components. In particular, VVV indicates the ceramic filter (KCF or ACF), WW indicates the pressure transducer (FD or CD), XXXX indicates the measuring range of the transducer in kPa (500 or 2000), YYYYY indicates the casing material (SS316 or Al) and, finally, Z indicates a design variant (1 or 2).

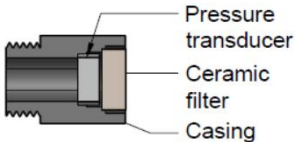
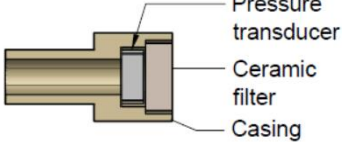
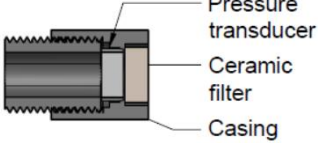
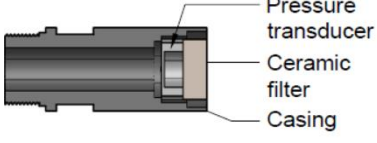
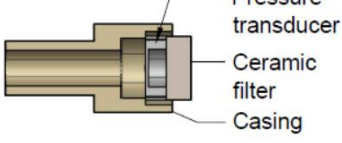
The first three prototypes in the first two rows of Table 4, i.e. KCF – FD(2000) – SS316 [1], ACF – FD(2000) – SS316 and KCF – FD(2000) – Al, were built around a flush diaphragm pressure transducer. In these three prototypes, the water reservoir was created via a special design of the casing, which incorporates a recess that is deeper than the height of the pressure transducer. The transducer fits inside the recess while the ceramic filter sits on the external edge of the recess, thus creating a small cylindrical gap between the transducer and the filter. This gap has a depth of 0.2 mm and a diameter of 16 mm, which results in a volume of about 40 mm<sup>3</sup>. The sides of both the transducer and the ceramic filter were sealed against the inner surface of the casing by means of an epoxy resin. The inner surface of the casing therefore delimits the perimeter of the reservoir.

The fourth prototype in the third row of Table 4, i.e. KCF – FD(2000) – SS316 [2], was built around a flush diaphragm pressure transducer likewise the previous three prototypes. The water reservoir was again created through a particular design of the casing, which includes a thin protruding lip that separates the ceramic filter from the transducer. The thickness of this lip creates a cylindrical gap between the filter and the transducer with a depth of 0.5 mm and a diameter of 10 mm, which results in a reservoir volume of about 40 mm<sup>3</sup>. A threaded adaptor was screwed on the back of the casing to push the pressure transducer against the protruding lip, thus securing it in place. The purpose of this design was to prevent any potential movement of the transducer when subjected to both negative (tensile) water pressures during measurements and positive (compressive) water pressures during saturation and calibration. Like the previous prototypes, the transducer and the ceramic filter were sealed against the inner sides of the casing by means of an epoxy resin.

The last three prototypes in the fourth and fifth rows of Table 4, i.e. KCF – CD(2000) – SS316, KCF – CD(2000) – Al and KCF – CD(500) – Al, were built around a cavity diaphragm pressure transducer. In these prototypes, the ceramic filter was directly sealed against the rim of the hollow transducer, whose inner cavity therefore delimited the base and the perimeter of the reservoir. The transducer cavity has a diameter of 10 mm and a depth of 5.5 mm resulting in a reservoir volume of about 430 mm<sup>3</sup>, which is more than ten times larger compared to the previous four prototypes. The cavity diaphragm transducer and the ceramic filter were glued together by means of an epoxy resin before being slotted as a single piece inside the casing where they were again sealed by means of an epoxy resin. In this case, unlike previous prototypes, the casing is not in direct contact with the water inside the reservoir. Note that the two prototypes KCF –

CD(2000) – AI and KCF – CD(500) – AI have identical appearances in Table 4 as they differ solely for the transducer full scale range, which is equal to 2000 kPa in the former case and 500 kPa in the latter case.

**Table 4.** Designs of HCT prototypes.

 <p>Pressure transducer Ceramic filter Casing</p>	<p><b>Name:</b> KCF – FD(2000) – SS316 [1] and ACF – FD(2000) – SS316</p> <p><b>Size:</b> 35 mm x <math>\varnothing</math>26 mm</p> <p><b>Ceramic filter:</b> KCF or ACF</p> <p><b>Water reservoir size:</b> 40mm<sup>3</sup> (0.2 mm x <math>\varnothing</math>16 mm)</p> <p><b>Pressure transducer:</b> 2000kPa ceramic flush diaphragm</p> <p><b>Casing material:</b> Stainless steel SS316</p> <p><b>Special feature:</b> Water reservoir included in the casing design</p>
 <p>Pressure transducer Ceramic filter Casing</p>	<p><b>Name:</b> KCF – FD(2000) – AI</p> <p><b>Size:</b> 50 mm x <math>\varnothing</math>26 mm</p> <p><b>Ceramic filter:</b> KCF</p> <p><b>Water reservoir size:</b> 40mm<sup>3</sup> (0.2 mm x <math>\varnothing</math>16 mm)</p> <p><b>Pressure transducer:</b> 2000kPa ceramic flush diaphragm</p> <p><b>Casing material:</b> Alumina ceramic</p> <p><b>Special feature:</b> Water reservoir included in the casing design</p>
 <p>Pressure transducer Ceramic filter Casing</p>	<p><b>Name:</b> KCF – FD(2000) – SS316 [2]</p> <p><b>Size:</b> 45 mm x <math>\varnothing</math>26 mm</p> <p><b>Ceramic filter:</b> KCF</p> <p><b>Water reservoir size:</b> 40mm<sup>3</sup> (0.5 mm x <math>\varnothing</math>10 mm)</p> <p><b>Pressure transducer:</b> 2000kPa ceramic flush diaphragm</p> <p><b>Casing material:</b> Stainless steel SS316</p> <p><b>Special features:</b> small lip in the casing design that separates ceramic filter and pressure transducer; use of a thread adaptor to secure the pressure transducer in place</p>
 <p>Pressure transducer Ceramic filter Casing</p>	<p><b>Name:</b> KCF – CD(2000) – SS316</p> <p><b>Size:</b> 60 mm x <math>\varnothing</math>26 mm</p> <p><b>Ceramic filter:</b> KCF</p> <p><b>Water reservoir size:</b> 430mm<sup>3</sup> (5.5 mm x <math>\varnothing</math>10 mm)</p> <p><b>Pressure transducer:</b> 2000kPa ceramic cavity diaphragm</p> <p><b>Casing material:</b> Stainless steel SS316</p> <p><b>Special feature:</b> cavity of the pressure transducer used as water reservoir</p>
 <p>Pressure transducer Ceramic filter Casing</p>	<p><b>Name:</b> KCF – CD(2000) – AI and KCF – CD(500) – AI</p> <p><b>Size:</b> 55 mm x <math>\varnothing</math>26 mm</p> <p><b>Ceramic filter:</b> KCF</p> <p><b>Water reservoir size:</b> 430mm<sup>3</sup> (5.5 mm x <math>\varnothing</math>10 mm)</p> <p><b>Pressure transducer:</b> 500kPa and 2000kPa ceramic cavity diaphragm</p> <p><b>Casing material:</b> Alumina ceramic</p> <p><b>Special feature:</b> cavity of the pressure transducer used as water reservoir</p>

## 4 Performance of HCT prototypes

The performance of the previous HCT prototypes was then compared in terms of the time required for saturation, the calibration accuracy in the positive pressure range and the maximum sustainable water tension.

### 4.1 Saturation and calibration of HCT prototypes

An adequate water saturation of both porous filter and reservoir is crucial for the good performance of HCTs during suction measurements. Two different saturation procedures were adopted in this work depending on whether the HCT was dry or “quasi-saturated” with only few small gas cavities in the porous filter and reservoir. The former saturation procedure is termed “first saturation” and is typically applied to a newly built HCT that is completely dry. The latter saturation procedure is instead termed “re-saturation” and is typically applied to an initially saturated HCT that has experienced cavitation during suction measurement leading to the formation of few small gas cavities inside the filter and reservoir. The gas cavities that have formed during cavitation must be eliminated to restore the sensor ability to record water tensions.

Marinho and Chandler (1994) suggested that the first saturation of HCTs should include the application of high vacuum followed by water flooding and pressurization. The application of high vacuum is necessary to minimize the amount of residual air inside the porous filter and reservoir prior to flooding while the subsequent pressurization helps dissolve any remaining gas cavities. Consistent with the above recommendations, a two stages procedure was adopted in this work for the first saturation of all HCTs. In the first stage, the filter was exposed to the vacuum created by a Pfeiffer DUO 11 two stage rotary vane vacuum pump delivering an ultimate absolute pressure of  $3 \cdot 10^{-4}$  kPa. During exposure to vacuum, the HCT readings were continuously monitored and stabilized after about 15 min. Once stabilization was achieved, the vacuum was maintained for a further hour to evacuate most of the entrapped air. The de-aired water line was then opened and the water, under atmospheric pressure, rapidly flooded the porous filter and reservoir. In the second stage, the water was compressed inside the HCT by means of a VJTech automatic pressure/volume controller capable of applying a maximum pressure of 2990 kPa. A compressive pressure of 2990 kPa was applied to all HCT prototypes except prototype KCF – CD(500) – A1, which was instead subjected to a lower pressure of 1000 kPa to avoid damaging the transducer. This was necessary because prototype KCF – CD(500) – A1 incorporates a transducer with a measuring range of 500 kPa instead of 2000 kPa like all other cases. A pressurization time between 12 and 24 hours was found to be sufficient to saturate the HCT prototypes with the smaller water reservoir built around a flush diaphragm transducer, namely KCF – FD(2000) – SS316 [1], KCF – FD(2000) – SS316 [2], ACF – FD(2000) – SS316 and KCF – FD(2000) – A1. A longer pressurization time up to 96hrs was instead necessary to saturate the HCT prototypes with the larger water reservoir built around a cavity pressure transducer, namely KCF – CD(2000) – SS316, KCF – CD(2000) – A1 and KCF – CD(500) – A1.

Instead, the re-saturation procedure involved a simple pressurization to either 2990 or 1000 kPa, depending on the measuring range of the pressure transducer, without any previous application of vacuum. This pressurization stage varied from minutes to hours depending on the time the HCT was left exposed to the atmosphere after cavitation. This procedure was found to be enough for restoring the ability of all HCTs to record negative pore-water pressures.

Calibration of all HCTs took place in the positive (compressive) pressure range and was subsequently linearly extrapolated to the negative (tensile) pressure range as discussed by Tarantino and Mongiovi (2003). A positive pressure cycle of 2990 kPa→50 kPa→2990 kPa was imposed to the HCT prototypes incorporating the transducers with a measuring range of 2000 kPa, namely KCF – FD(2000) – SS316 [1], KCF – FD(2000) – SS316 [2], ACF – FD(2000) – SS316, KCF – FD(2000) – A1, KCF – CD(2000) – SS316 and KCF – CD(2000) – A1. A smaller pressure cycle of 1000 kPa→50 kPa→1000 kPa was instead imposed to the single HCT prototype incorporating a pressure transducer with a measuring range of 500 kPa, namely

KCF – CD(500) – Al. The maximum pressure applied during calibration was higher than the full scale range but smaller than the overload limit to avoid damaging the transducer. The application of such extreme pressure levels was helpful to explore the linearity of the transducer response even beyond the full scale range. The results of the different calibrations are summarized in Figure 4, which shows the relationship between pressure and voltage for all HCT prototypes. Inspection of Figure 4 indicates that, regardless of reservoir size, ceramic filter and transducer type, all HCT prototypes exhibit a linear response over the applied pressure range with a negligible hysteresis of 0.04%. This result confirms that the applied pressure can be safely pushed beyond the full scale range, provided that the overpressure limit is not exceeded, thus achieving a reasonable compromise between accuracy and pre-pressurisation as discussed in Section 3.2.

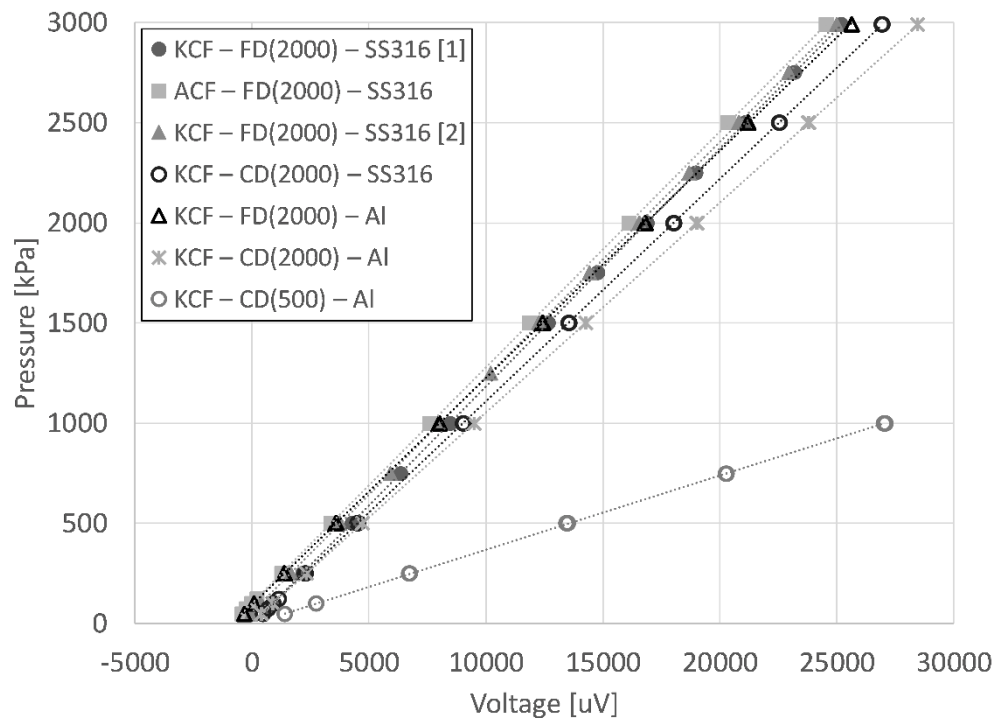


**Figure 4.** Calibration curves of HCT prototypes.

#### 4.2 Maximum sustainable water tension of HCT prototypes

All HCT prototypes were subjected to evaporation tests to determine their respective maximum sustainable water tensions or, in other words, their respective measuring ranges. During these tests, the HCT prototypes were exposed to the atmosphere, thus allowing the progressive depletion of water from the menisci at the outer face of the filter. This evaporation generates an increasingly larger water tension inside the saturated filter, which propagates almost instantaneously to the reservoir causing the inward deflection of the transducer diaphragm. The HCT therefore reads increasingly larger water tensions (i.e. negative water pressures) until a sudden breakdown of measurements occurs leading to an instantaneous rise of pressure to about -100 kPa, which is close to the water vapour gauge pressure. This breakdown of measurements corresponds to the expansion of small gas cavities inside the water reservoir and is commonly termed “cavitation”. The lowest (negative) water pressure recorded immediately before cavitation is here taken as the maximum sustainable water tension.

Prototypes KCF – FD(2000) – SS316 [1] and ACF – FD(2000) – SS316 have identical pressure transducers, reservoir sizes, and protective casings but different ceramic filters. By comparing the results from their

respective evaporation tests, it is therefore possible to evaluate the effects of the KCF (whose nominal AEV is 1.5 MPa) and the ACF (whose estimated AEV is 1.0 MPa) on the maximum sustainable water tension. Figure 5 shows the results from a typical evaporation test for each of these two prototypes and indicates that the prototype incorporating the KCF attains a lower water pressure before cavitation (about -2000 kPa) compared to the prototype incorporating the ACF (about -700 kPa). This is consistent with the data shown in Figure 2 and Table 1, which indicate that the KCF exhibits a smaller pore size and, hence, a larger AEV than the ACF. The prototype incorporating the KCF can therefore sustain higher water tensions compared to the prototype incorporating the ACF. The use of the ACF may however still be preferable in harsh field conditions, where robustness is important, because of its higher density and hardness (Table 2).

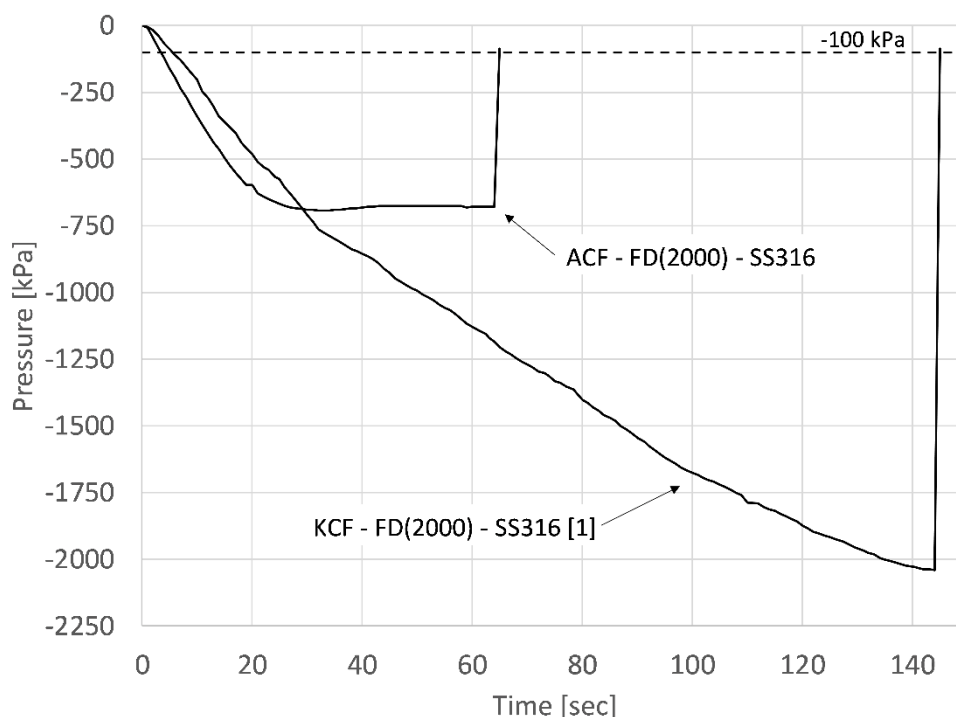


**Figure 5.** Typical evaporation tests on identical prototypes incorporating different ceramic filters (ACF – FD(2000) – SS316 and KCF – FD(2000) – SS316 [1]).

Given the larger AEV of the KCF compared to the ACF, six out of the seven prototypes manufactured in the present work incorporated the KCF. Figure 6 shows the results from one typical evaporation test for each of these six prototypes while Table 5 presents the minimum water pressures registered just before cavitation during five distinct evaporation tests for each prototype. Inspection of Figure 6 and Table 5 indicates that, regardless of reservoir size, pressure transducer and protective casing, the ultimate water pressure recorded before cavitation is always lower than -1500 kPa.

The only exception is given by prototype KCF – CD(500) – Al, which incorporates a pressure transducer with a full scale range of 500 kPa instead of 2000 kPa. As previously discussed, the smaller full scale range required the application of a lower positive pressure (1000 kPa) during saturation and calibration of this prototype to prevent damaging the transducer. This might have hampered the dissolution of air cavities inside the ceramic filter and water reservoir, which is the reason why the maximum tension is lower compared to the other prototypes. It is however worth highlighting that, despite the low pre-pressurisation, prototype KCF – CD(500) – Al was still capable of measuring significant water tensions, up to about -1300 kPa, which is even larger than the overload limit of the transducer (1000 kPa). It was later checked that calibration had not changed despite the relatively large value of the maximum measured tension. Therefore,

if high accuracy is required especially in the low suction range, a transducer with a smaller full scale can possibly be employed.

Figure 6 shows that the evaporation rate is approximately similar for all prototypes and that the time to cavitation ranges between 50 and 140 seconds. The only exception to this behaviour is provided by prototype KCF – CD(2000) – SS316, which exhibits a significantly slower evaporation rate taking about 260 seconds to reach cavitation. The slower response of this prototype was initially attributed to its relatively large reservoir size but this hypothesis was subsequently disproved by the tests on prototype KCF – CD(2000) – Al, which has an identical reservoir size but exhibits a faster response. Prototypes KCF – CD(2000) – SS316 and KCF – CD(2000) – Al are virtually identical with the only difference being the material of the casing which should, however, have no effect as the casing is not in direct contact with the water inside the reservoir (Table 4).

It was later speculated that the different behaviour of prototypes KCF – CD(2000) – Al and KCF – CD(2000) – SS316 might have been caused by the different epoxy resins used to assemble the two prototypes. In particular, an epoxy resin for ceramics and metals was used to assemble the KCF – CD(2000) – Al prototype while an epoxy resin for casting/potting was employed to assemble the KCF – CD(2000) – SS316 prototype. Note, however, that the stiffnesses of the two resins are very similar, i.e. 2400 MPa in the former case compared to 2900 MPa in the latter case, which suggests that an explanation should rather be found in the different chemical properties of the resins, though this hypothesis requires further investigation.

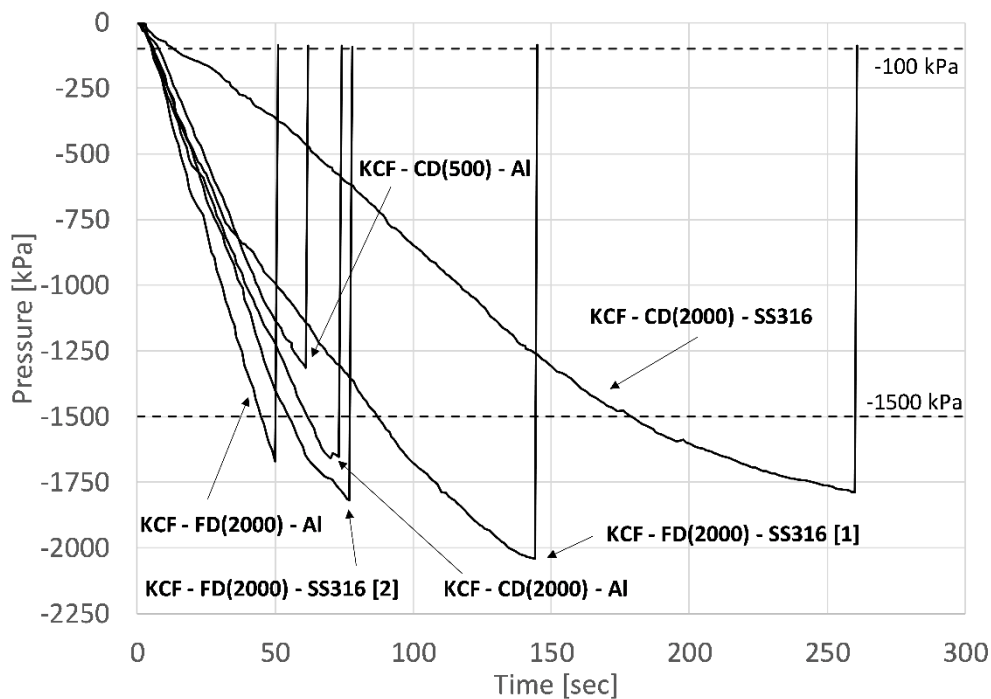


**Figure 6.** Typical evaporation tests on different prototypes incorporating identical ceramic filters (KCF).



**Table 5.** Water tensions recorded during multiple tests on different HCT prototypes just before cavitation.

HCT prototype	KCF FD(2000) SS316 [1]	KCF FD(2000) Al	KCF FD(2000) SS316 [2]	KCF CD(2000) SS316	KCF CD(2000) Al	KCF CD(500) Al
	Recorded cavitation pressure [kPa]	-1563	-1582	-1676	-1641	-1605
-1642		-1603	-1677	-1718	-1646	-1284
-1669		-1623	-1699	-1735	-1666	-1302
-1896		-1788	-1735	-1774	-1754	-1305
-2041		-1965	-1819	-1976	-1932	-1314

## 5 Conclusions

This article has discussed the effect of sensor design on the saturation, calibration and maximum measurable water tension of High Capacity Tensiometers (HCTs). In particular, the study has compared the performance of seven distinct HCT incorporating different pressure transducers, porous filters, water reservoir sizes, protective casings and epoxy resins.

Among all design variables, the air entry value (AEV) of the porous filter appears to have the strongest influence on the maximum water tension recorded by the HCTs and, hence, on their measuring range. Evaporation tests showed that the maximum water tension, measured just before cavitation, was larger when the AEV of the filter was bigger, thus confirming past evidence that a properly saturated HCT is generally capable of measuring a maximum tension close to the AEV of the filter. In particular, the HCT prototypes incorporating a kaolin ceramic filter with an AEV of 15 bar measured a maximum water tension between -1800 kPa and -2000 kPa while the HCT prototypes incorporating an alumina ceramic filter with an AEV between 7 and 10 bar measured a maximum water tension between -700 kPa and -800 kPa. Moreover, the analysis of results from porosimetry tests on both ceramic filters confirmed that the AEV is inversely related to the size of the largest pore in the filter.

Contrary to common belief, the size of the water reservoir does not seem to affect the response time of HCTs during evaporation tests, nor does it influences the maximum water tension recorded before cavitation. This may be because cavitation is triggered by gas nuclei that are either located in the porous filter (Mendes and Buzzi, 2013) or on the reservoir surface which, unlike the reservoir volume, did not change significantly between prototypes. It is however still unclear whether the reservoir size influences the long-term performance of HCTs and the stability of measurements over time. This is an important aspect to consider for field monitoring applications and is the object of a companion paper (Mendes and Gallipoli, 2020). Special consideration should also be given to the process of fabricating HCTs and to the type of epoxy resin used to assemble the sensor components, especially if the resin is in direct contact with the water inside the sensor.

Consistent with past studies, this work indicates that the procedures for the first saturation and re-saturation of HCTs can have a significant influence on the measuring performance of the sensors. In particular, the application of a large positive pressure may considerably increase the maximum sustainable water tension. This is evident by comparing the results from the evaporation tests performed on two similar prototypes subjected to different saturation pressures of 1000 kPa and 2990 kPa, respectively. The maximum water tension recorded by the former prototype was about 25% smaller than the maximum tension recorded by the latter prototype.

## Acknowledgements

The financial contribution of the European Commission to this research through the Marie Curie Industry-Academia Partnership and Pathways Network MAGIC (Monitoring systems to Assess Geotechnical Infrastructure subjected to Climatic hazards) – PIAPP-GA-2012-324426 – is gratefully acknowledged.

## References

- Bagheri, M., Rezaei M. and Mousavi Nezhad M., 2018. Cavitation in high-capacity tensiometers: effect of water reservoir surface roughness. *Geotechnical Research* 5(2): 81–95.
- Barrett, E.P., Joyner, L.G., Halenda, P.P., 1951. The determination of pore volume and area distributions in porous substances. I. Computations from nitrogen isotherms *J. Am. Chem. Soc.* 73: 373–380.
- Delage, P., Romero, E. and Tarantino, A. 2008. Keynote Lecture: Recent developments in the techniques of controlling and measuring suction. *Proc. 1st European Conference on Unsaturated Soils*, 2-4th July 2008, Durham, UK: 33-52.
- Caruso, A., Tarantino, A., 2004. A shearbox for testing unsaturated soils from medium to high degrees of saturation. *Geotechnique* 54(4):281-284.
- Cui, Y.J., Tang, A., Mantho, A., De Laure, E., 2008. Monitoring field soil suction using a miniature tensiometer. *Geotechnical Testing Journal* 31(1): 95-100.
- Cunningham, M. R., Ridley, A. M., Dineen, K. and Burland, J. B. 2003. The mechanical behaviour of a reconstituted unsaturated silty clay. *Géotechnique*, 53: 183-194.
- Giesche, H., 2006. Mercury porosimetry: a general (practical) overview. *Part. Part. Syst. Charact.*, 23:9-19.
- Guan, Y., Fredlund, D.G., 1997. Use of the tensile strength of water for the direct measurement of high soil suction. *Canadian Geotechnical Journal*, 34(4): 604-614.
- Le, T.T., Cui, Y.J. and Muñoz, J., Delage, P., Tang, A.M. and Li, X.L., (2011). Studying the stress-suction coupling in soils using an oedometer equipped with a high capacity tensiometer. *Frontiers of Architecture and Civil Engineering in China*. 5. 160-170. 10.1007/s11709-011-0106-x.
- Lourenço, S.D.N., Gallipoli, D., Toll, D.G., Augarde, C., Evans, F., Medero, G.M., 2008. Calibration of a high-suction Tensiometer. *Géotechnique* 58(8): 659-668.
- Marinho, F.A.M., Chandler, R.J., 1994. Discussion on A new instrument for the measurement of soil moisture suction. *Géotechnique* 44(3): 551-556.
- Marinho, F.A.M., and de Sousa Pinto, C. (1997). Soil suction measurement using a tensiometer. *Symposium on Recent Development in Soil and Pavement Mechanics - Rio de Janeiro*, June. pp. 249-254.
- Marinho F.A.M., Take A. and Tarantino A. 2008. Tensiometric and axis translation techniques for suction measurement. *Geotechnical and Geological Engineering*, 26(6): 615-631.
- Meilani, I., Rahardjo, H., Leong, E.C., Fredlund, D.G., 2002. Mini suction probe for matric suction measurements. *Canadian Geotechnical Journal* 39: 1427-1432.
- Mendes, J., Buzzi, O., 2013. New insight into cavitation mechanisms in high-capacity tensiometers based on high-speed photography. *Canadian Geotechnical Journal* 50(5): 550-556.
- Mendes, J., Buzzi, O., 2014. Performance of the University of Newcastle high capacity tensiometers. *Proc. UNSAT 2014, Unsaturated Soils: Research and Applications*, Sydney Australia: 1611-1616.

- Mendes, J., Gallipoli, D., 2020. Comparison of high capacity tensiometer designs for the long-term measurements of soil suction. *Physics and Chemistry of the Earth*, 115: 102831. <https://doi.org/10.1016/j.pce.2019.102831>
- Mendes, J., Gallipoli, D., Plantier, F., Gregoire, D., 2015. Filtres de ceramique pour tensiometres a haute capacite. In *Proceedings Rencontres Universitaires de Genie Civil, Bayonne, France*.
- Mendes, J., Toll, D.G., 2016. Influence of initial water content on the mechanical behaviour of unsaturated sandy clay soil. *Int J Geomech* 16(6):D4016005
- Mendes, J., Toll, D.G., Augarde, C.E., Gallipoli, D., 2008. A system for field measurement of suction using high capacity tensiometers. In *Unsaturated Soils: Advances in Geo-Engineering, Proceedings 1st European Conference on Unsaturated Soils, Durham, United Kingdom*, 219-225.
- Ridley, A.M., Burland, J.B., 1993. A new instrument for the measurement of soil moisture suction. *Géotechnique* 43(2): 321-324.
- Take, W.A., Bolton, M.D., 2003. Tensiometer saturation and the reliable measurement of soil suction. *Géotechnique* 54(3): 159-172.
- Tarantino, A., Mongiovì, L., 2001. Experimental procedures and cavitation mechanisms in tensiometer measurements. *Geotech. Geol. Engng* 19, No. 3, 191–210.
- Tarantino, A., Mongiovì, L., 2002. Design and construction of a tensiometer for direct measurement of matric suction. In *Proceedings 3rd International Conference on Unsaturated soils, Recife, Brazil*, 1: 319-324.
- Tarantino, A. and Mongiovì, L. (2003). Calibration of tensiometer for direct measurement of matric suction. *Géotechnique*, Technical Note, 53, No.1, 137-141.
- Tarantino A. and De Col E. 2008. Compaction behaviour of clay. *Géotechnique* 58(3): 199–213.
- Toll D.G., Lourenço S.D.N. Mendes J., Gallipoli D., Evans F.D., Augarde C.E., Cui Y.J., Tang A.M., Rojas J.C., Pagano, L. Mancuso C., Zingariello C. and Tarantino A. 2011. Soil suction monitoring for landslides and slopes. *Quarterly Journal of Engineering Geology and Hydrogeology*, 44, 1–13. DOI 10.1144/1470-9236/09-010
- Toker, N. K., Germaine, J. T., Sjoblom, K. J. ve Culligan, P. J. (2004). "A new technique for rapid measurement of continuous soil moisture characteristic curves", *Géotechnique*, Vol.54, No.3, p.179-186.
- Wijaya, Martin and Leong, E. (2016). Performance of high-capacity tensiometer in constant water content oedometer test. *International Journal of Geo-Engineering*. 7. 13. 10.1186/s40703-016-0027-6.
- Zheng, Q., Durben, D.J., Wolf, G.H., Angell, C.A., 1991. Liquids at large negative pressure: water at the homogeneous nucleation limit. *Science*: 254: 829-832.

**List of tables:****Table 1.** Ceramic filter properties.

	<b>Pore size range nm</b>	<b>Largest pore nm</b>	<b>Porosity %</b>	<b>Specific density g/cm<sup>3</sup></b>	<b>Bulk density g/cm<sup>3</sup></b>
KCF	2 - 220	165 - 220	33	2.02	1.35
ACF	100 - 290	250 - 290	13	3.10	2.70

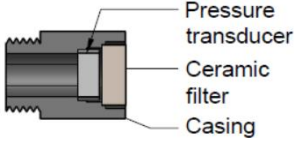
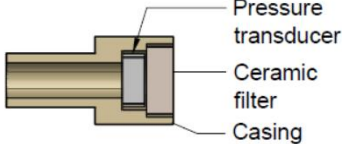
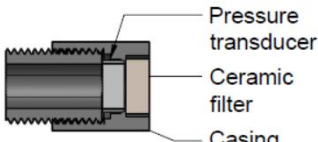
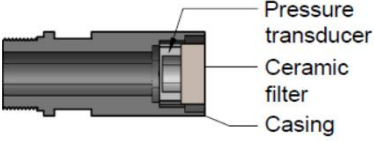
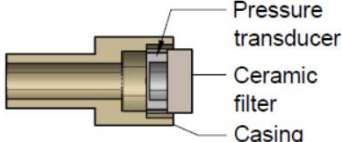
**Table 2 –** Pressure transducer characteristics.

<b>Designation</b>	Ceramic flush diaphragm	Ceramic cavity diaphragm
<b>Short name</b>	FD	CD
<b>Sensor type</b>	Piezoresistive	
<b>Pressure reference</b>	Relative to atmosphere	Relative to atmosphere
<b>Pressure full scale range (FS) [kPa]</b>	2000	500 / 2000
<b>Accuracy [%FS]</b>	0.5	

**Table 3.** Main properties of casing materials.

		<b>SS316</b>	<b>Al</b>
<b>Thermal coefficient of linear expansion</b>	<b>[10<sup>-6</sup> K<sup>-1</sup>]</b>	16	8
<b>Thermal conductivity at 25°C</b>	<b>[W/(m.K)]</b>	16	35
<b>Specific heat</b>	<b>[J/(kg.K)]</b>	500	880
<b>Stiffness (Young modulus)</b>	<b>GPa</b>	200	360

**Table 4.** Designs of HCT prototypes.

 <p>Pressure transducer Ceramic filter Casing</p>	<p><b>Name:</b> KCF – FD(2000) – SS316 [1] and ACF – FD(2000) – SS316</p> <p><b>Size:</b> 35 mm x <math>\varnothing</math>26 mm</p> <p><b>Ceramic filter:</b> KCF or ACF</p> <p><b>Water reservoir size:</b> 40mm<sup>3</sup> (0.2 mm x <math>\varnothing</math>16 mm)</p> <p><b>Pressure transducer:</b> 2000kPa ceramic flush diaphragm</p> <p><b>Casing material:</b> Stainless steel SS316</p> <p><b>Special feature:</b> Water reservoir included in the casing design</p>
 <p>Pressure transducer Ceramic filter Casing</p>	<p><b>Name:</b> KCF – FD(2000) – Al</p> <p><b>Size:</b> 50 mm x <math>\varnothing</math>26 mm</p> <p><b>Ceramic filter:</b> KCF</p> <p><b>Water reservoir size:</b> 40mm<sup>3</sup> (0.2 mm x <math>\varnothing</math>16 mm)</p> <p><b>Pressure transducer:</b> 2000kPa ceramic flush diaphragm</p> <p><b>Casing material:</b> Alumina ceramic</p> <p><b>Special feature:</b> Water reservoir included in the casing design</p>
 <p>Pressure transducer Ceramic filter Casing</p>	<p><b>Name:</b> KCF – FD(2000) – SS316 [2]</p> <p><b>Size:</b> 45 mm x <math>\varnothing</math>26 mm</p> <p><b>Ceramic filter:</b> KCF</p> <p><b>Water reservoir size:</b> 40mm<sup>3</sup> (0.5 mm x <math>\varnothing</math>10 mm)</p> <p><b>Pressure transducer:</b> 2000kPa ceramic flush diaphragm</p> <p><b>Casing material:</b> Stainless steel SS316</p> <p><b>Special features:</b> small lip in the casing design that separates ceramic filter and pressure transducer; use of a thread adaptor to secure the pressure transducer in place</p>
 <p>Pressure transducer Ceramic filter Casing</p>	<p><b>Name:</b> KCF – CD(2000) – SS316</p> <p><b>Size:</b> 60 mm x <math>\varnothing</math>26 mm</p> <p><b>Ceramic filter:</b> KCF</p> <p><b>Water reservoir size:</b> 430mm<sup>3</sup> (5.5 mm x <math>\varnothing</math>10 mm)</p> <p><b>Pressure transducer:</b> 2000kPa ceramic cavity diaphragm</p> <p><b>Casing material:</b> Stainless steel SS316</p> <p><b>Special feature:</b> cavity of the pressure transducer used as water reservoir</p>
 <p>Pressure transducer Ceramic filter Casing</p>	<p><b>Name:</b> KCF – CD(2000) – Al and KCF – CD(500) – Al</p> <p><b>Size:</b> 55 mm x <math>\varnothing</math>26 mm</p> <p><b>Ceramic filter:</b> KCF</p> <p><b>Water reservoir size:</b> 430mm<sup>3</sup> (5.5 mm x <math>\varnothing</math>10 mm)</p> <p><b>Pressure transducer:</b> 500kPa and 2000kPa ceramic cavity diaphragm</p> <p><b>Casing material:</b> Alumina ceramic</p> <p><b>Special feature:</b> cavity of the pressure transducer used as water reservoir</p>

**Table 5.** Water tensions recorded by different HCT prototypes just before cavitation.

<b>HCT prototype</b>	<b>KCF FD(2000) SS316 [1]</b>	<b>KCF FD(2000) Al</b>	<b>KCF FD(2000) SS316 [2]</b>	<b>KCF CD(2000) SS316</b>	<b>KCF CD(2000) Al</b>	<b>KCF CD(500) Al</b>
<b>Recorded cavitation pressure [kPa]</b>	-1563	-1582	-1676	-1641	-1605	-1256
	-1642	-1603	-1677	-1718	-1646	-1284
	-1669	-1623	-1699	-1735	-1666	-1302
	-1896	-1788	-1735	-1774	-1754	-1305
	-2041	-1965	-1819	-1976	-1932	-1314